

MAST/Orbit has a role in microtubule–kinetochore attachment and is essential for chromosome alignment and maintenance of spindle bipolarity

Helder Maiato,^{2,3} Paula Sampaio,² Catarina L. Lemos,² John Findlay,⁴ Mar Carmena,³ William C. Earnshaw,³ and Claudio E. Sunkel^{1,2}

¹Instituto de Ciências Biomédicas de Abel Salazar and ²Laboratório de Genética Molecular, Instituto de Biologia Molecular e Celular, Universidade do Porto, 4150-180 Porto, Portugal

³Chromosome Structure Group, Wellcome Trust Centre for Cell Biology and ⁴Biological Sciences Electron Microscope Facility, Institute of Cell and Molecular Biology, University of Edinburgh, Scotland, UK

Multiple asters (MAST)/Orbit is a member of a new family of nonmotor microtubule-associated proteins that has been previously shown to be required for the organization of the mitotic spindle. Here we provide evidence that MAST/Orbit is required for functional kinetochore attachment, chromosome congression, and the maintenance of spindle bipolarity. In vivo analysis of *Drosophila mast* mutant embryos undergoing early mitotic divisions revealed that chromosomes are unable to reach a stable metaphase alignment and that bipolar spindles collapse as centrosomes move progressively closer toward the cell center and eventually organize into a monopolar configuration. Similarly, soon after depletion of MAST/Orbit in *Drosophila* S2 cells by double-stranded RNA interference, cells are unable to form a metaphase plate and instead

assemble monopolar spindles with chromosomes localized close to the center of the aster. In these cells, kinetochores either fail to achieve end-on attachment or are associated with short microtubules. Remarkably, when microtubule dynamics is suppressed in MAST-depleted cells, chromosomes localize at the periphery of the monopolar aster associated with the plus ends of well-defined microtubule bundles. Furthermore, in these cells, dynein and ZW10 accumulate at kinetochores and fail to transfer to microtubules. However, loss of MAST/Orbit does not affect the kinetochore localization of D-CLIP-190. Together, these results strongly support the conclusion that MAST/Orbit is required for microtubules to form functional attachments to kinetochores and to maintain spindle bipolarity.

Introduction

The mitotic spindle, a highly dynamic structure composed of microtubules and associated proteins, is essential for chromosome segregation during mitosis. Temporal and spatial coordination of spindle-associated proteins regulates many aspects of this structure including centrosome separation, formation and maintenance of bipolarity, and the alignment and segregation of the chromosomes (for review see Sharp et al., 2000b). Spindle proteins can be divided into three groups, microtubule-based motor proteins, microtubule-destabilizing factors, and nonmotor microtubule-associated

proteins (MAPs),* mostly having a role in the stabilization of microtubules.

The role of multiple microtubule motors in spindle assembly has been the subject of intense investigation (for review see Hoyt and Geiser, 1996). Pioneering work in budding yeast showed that disruption of the balance of kinesin motors resulted in rapid collapse of the spindle (Saunders et al., 1997). Subsequent studies in *Drosophila* embryos have shown that spindle assembly, maintenance, and elongation depend upon the coordinated activity of motors including bipolar kinesins, COOH-terminal kinesins, and cytoplasmic dynein (Sharp et al., 2000a). Dynein is thought to anchor astral microtubules to the cell cortex and, through its minus

The online version of this article includes supplemental material.

Address correspondence to Claudio E. Sunkel, Instituto de Biologia Molecular e Celular, Universidade do Porto, Rua do Campo Alegre 823, 4150-180 Porto, Portugal. Tel.: 351-22-607-4900. Fax: 351-22-609-9157. E-mail: cesunkel@ibmc.up.pt

H. Maiato and P. Sampaio contributed equally to this work.

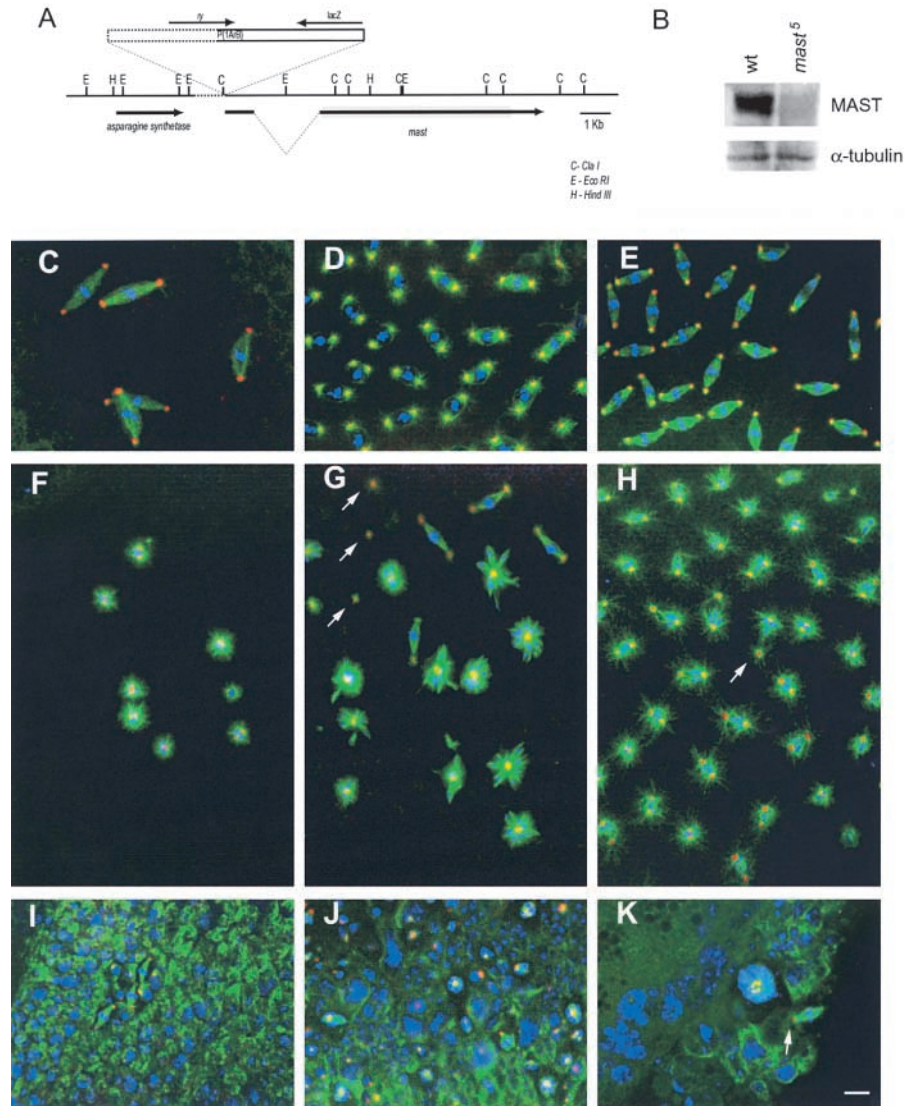
Key words: MAST; microtubules; kinetochores; spindle; *Drosophila*

*Abbreviations used in this paper: ds, double stranded; GFP, green fluorescent protein; MAP, microtubule-associated protein; MAST, multiple asters; RNAi, dsRNA-mediated interference; NEB, nuclear envelope breakdown.

Supplemental Material can be found at:
<http://jcb.rupress.org/content/suppl/2002/05/23/jcb.200201101.DC1.html>

Figure 1. Characterization of *mast⁵*.

(A) Schematic representation of the deletion (dotted line) associated with the *mast⁵* allele. The gray box represents the open reading frame of *mast*. (B) Western blot analysis of wild-type and *mast⁵* embryos. α -Tubulin levels are shown as a loading control. Wild-type (C–E) or *mast⁵* (F–K) embryos were immunostained to reveal the spindle and centrosomes by antibody detection of α -tubulin (green) and centrosomin (red) respectively, and DNA was counterstained with DAPI (blue). Wild-type embryos during early (C) and late (D and E) embryogenesis show well-organized bipolar spindles with centrosomes at both poles. (F) Early syncytial *mast⁵* embryo (eight nuclei) showing monopolar spindles. (G) *mast⁵* embryo showing monopolar spindles with chromosomes associated with the aster. Mutant embryos also show isolated centrosomes (arrows) and a few well-organized bipolar spindles with highly condensed chromosomes. (H) *mast⁵* embryo showing very short bipolar spindles and bipolar spindles with centrosomes in a single pole (arrow). (I) Postcellularized wild-type embryo showing a mitotic domain. (J) Late *mast⁵* embryo showing highly abnormal mitotic domains with polyploid cells containing monopolar spindles organized from clusters of centrosomes. (K) Part of a cellularized embryo with a large polyploid cell and another cell with a bipolar spindle with centrosomin staining in a single pole (arrow). Bar, 10 μ m.



end-directed motor activity, maintain spindle pole positioning and promote spindle elongation. Dynein also localizes to kinetochores during mitosis (Pfarr et al., 1990) and might be involved in chromosome segregation during anaphase (Sharp et al., 2000c).

More recently, significant advances have been made in analyzing the function of nonmotor MAPs like the conserved Dis1-TOG family (for review see Ohkura et al., 2001). These MAPs have been shown to localize mainly to the centrosomes and spindle microtubules during mitosis. Biochemical studies have shown that Dis1-TOG proteins promote microtubule stability by stimulating growth at the plus end. Genetic analysis indicated that they are required for spindle organization and might regulate the balance of forces during the metaphase–anaphase transition. A more direct role in the stabilization of microtubule–kinetochore interactions has also been proposed for the *Schizosaccharomyces pombe* homologue Dis1, as well as for its *Saccharomyces cerevisiae* homologue Stu2p (Garcia et al., 2001; He et al., 2001; Nakaseko et al., 2001). These proteins associate transiently with kinetochores during mitosis, however, only Dis1 appears to bind kinetochores independently of microtubules. The failure of

sister chromatid separation observed in *dis1* and *STU2* mutant cells has been associated with defects in the formation/stabilization of kinetochore microtubules. Fission yeast contain a second highly related protein, Alp14, that is required not only for overall microtubule assembly but also for the spindle assembly checkpoint (Shah and Cleveland, 2000; Garcia et al., 2001; Nigg, 2001). Experiments in *S. cerevisiae* have shown that kinetochore assembly is required for checkpoint function (Goh and Kilmartin, 1993), and it is possible that Alp14 may mediate the microtubule attachment to kinetochores that is monitored by the checkpoint.

Multiple asters (MAST)/Orbit defines another emergent family of nonmotor MAPs that contains an NH₂-terminal domain also present in the Dis1-TOG family (Inoue et al., 2000; Lemos et al., 2000). The MAST/Orbit family includes the human and mouse CLASPs (Akhmanova et al., 2001) and *S. cerevisiae* Stu1p (Pasqualone and Huffaker, 1994). One homologue in *S. pombe* and three in *Caenorhabditis elegans* were also identified by sequence similarity but remain uncharacterized (Lemos et al., 2000). Although no mitotic function has yet been described for CLASPs, these proteins were identified by their capacity to bind CLIP-170,

a protein originally identified through its ability to link endocytic vesicles to microtubules (Pierre et al., 1992), and later shown to localize to kinetochores of prometaphase chromosomes (Dujardin et al., 1998). MAST/Orbit and Stu1p are essential for spindle assembly (Pasqualone and Huffaker, 1994; Inoue et al., 2000; Lemos et al., 2000). During mitosis, MAST is localized to the mitotic spindle, centrosomes, and kinetochores, accumulates in the central spindle region, and ultimately concentrates at the midbody. Mutations in *mast* show severe mitotic abnormalities, including the formation of mono- and multipolar spindles organized by clusters of centrosomes (Lemos et al., 2000).

To further elucidate the function of MAST/Orbit during mitosis, we performed an *in vivo* analysis of mitotic progression in *mast* mutant embryos and a time course analysis of mitosis after double-stranded (ds) RNA-mediated interference (RNAi) of MAST/Orbit in *Drosophila* tissue culture cells. We found that MAST/Orbit is required for proper chromosome congression during prometaphase and for the stability of the bipolar spindle. Furthermore, we show that after depletion of MAST by dsRNAi, cells mostly organize monopolar spindles, and kinetochores fail to associate with the plus ends of microtubules. These observations suggest that MAST/Orbit has a role in microtubule-kinetochore attachment and maintenance of spindle bipolarity.

Results

Characterization of *mast*⁵, a new hypomorphic allele

We have identified and characterized a new female sterile mutant allele of MAST (*mast*⁵) that allowed us to monitor *in vivo* the effects of the loss of MAST function during mitotic progression in early *Drosophila* embryos. *mast*⁵ was obtained by imprecise excision of the P element present in *mast*¹ (Lemos et al., 2000) and has a partial deletion of the 5' end of the P element and ~1 kb of *mast* sequence upstream of the P element insertion site. Neither the upstream gene (*asparagine synthetase*) nor the *mast* sequences downstream of the insertion site are affected by the deletion (Fig. 1 A). Immunoblotting analysis showed that the levels of MAST in embryos laid by *mast*⁵ females (designated as *mast*⁵ embryos) are significantly reduced as compared with the wild-type control (Fig. 1 B).

Immunofluorescence analysis of wild-type embryos revealed the formation of bipolar spindles with one centrosome at each pole and the chromosomes aligned in the equatorial region during metaphase at successive stages of nuclear multiplication (Fig. 1, C–E). In contrast, mutant embryos in early (Fig. 1 F) or late (Fig. 1, G–K) mitotic cycles were characterized by the presence of monopolar spindles organized from one or two centrosomal foci with chromosomes dispersed within the aster (Fig. 1, F and G). Bipolar spindles and isolated centrosomes were also regularly observed (Fig. 1 G), as well as short bipolar spindles with the poles close to the chromosomes (Fig. 1 H). Cellularized mutant embryos were characterized by the presence of highly polyploid cells that, in mitosis, organize monopolar or bipolar spindles with centrosomes at a single pole (Fig. 1, I–K). Thus, *mast*⁵ is a hypomorphic mutation with an embryonic phenotype very similar to the one previously described in larval neuroblasts (Lemos et al., 2000).

In vivo analysis of mitotic progression in *mast*⁵ mutant embryos

To analyze the *in vivo* behavior of the mitotic apparatus in MAST-deficient embryos, we introduced a GFP-Polo transgene (Moutinho-Santos et al., 1999) into the *mast*⁵ line. The GFP-Polo protein is fully functional and was shown to be a good marker for centrosomes, mitotic spindle, kinetochores, and the midbody during early embryonic development. Embryos at nuclear cycle 12 laid by *gfp-polo* (control) and *gfp-polo;mast*⁵ females were observed by time-lapse confocal microscopy. Representative frames are displayed in Fig. 2 A and supplemental movies can be viewed at <http://www.jcb.org/cgi/content/full/jcb.200201101/DC1>. GFP-Polo localizes to the kinetochores at nuclear envelope breakdown (NEB), enabling us to follow chromosome movement from prometaphase onward (Fig. 2 A, 0 s). In control embryos, chromosomes became rapidly associated with spindle microtubules and soon established a metaphase plate (Fig. 2 A, 80–320 s). Time-lapse analysis of *mast*⁵ embryos shows that during early stages of mitosis, the centrosomes separated as in controls and a bipolar spindle was assembled after NEB (Fig. 2 A, –250–80 s). However, during prometaphase, chromosomes never reached a stable position at the equatorial region and appeared instead to drift back and forth along spindle microtubules (Fig. 2 A, 80–320 s).

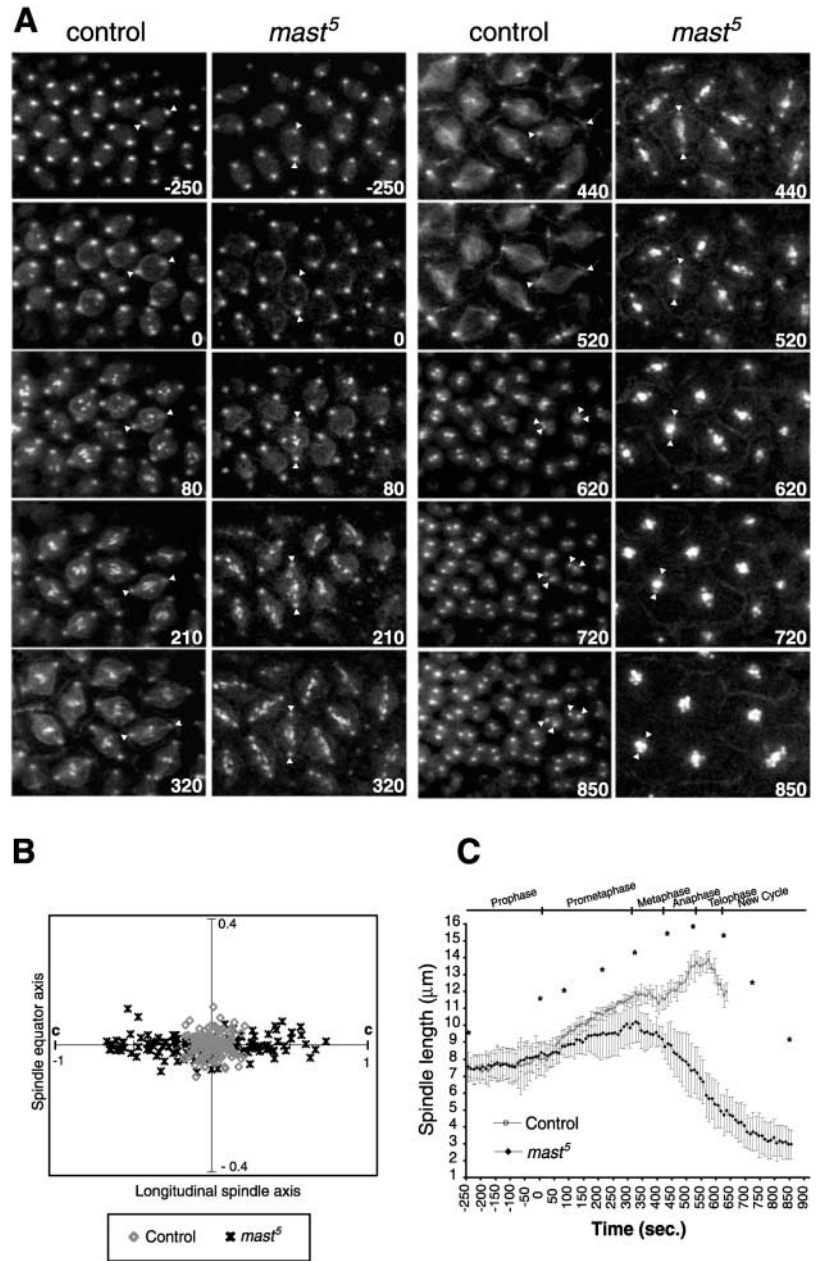
We quantified the chromosome congression defect by determining the localization of the GFP-Polo kinetochore signal in wild-type and *mast*⁵ mutant chromosomes at the time of metaphase (Fig. 2 B). By contouring, we could define the average area of the metaphase plate occupied by >95% of the centromeres in control cells. In *mast*⁵ embryos, only 32% of centromeres were able to cluster within an equivalent area. These data demonstrate that in the absence of MAST/Orbit, chromosomes are unable to reach a stable metaphase alignment.

To determine the effects of the *mast*⁵ mutation on mitotic spindle dynamics, we measured the centrosome-to-centrosome distance as a function of time in control and *mast*⁵ embryos, taking as a reference point the initiation of NEB (Fig. 2 C, 0 s). Centrosomes in *mast*⁵ embryos separated normally during prophase. However, during prometaphase, mutant embryos were unable to extend the spindle as in controls, indicating some role for MAST in spindle elongation at this stage. During metaphase in control embryos, the spindle length was initially constant and then had a slight decrease. During this stage, the spindles in *mast*⁵ embryos started to shorten and ended up collapsing toward the equatorial region, leading to the formation of monopolar spindles (Fig. 2 A, 440–850 s). These results provide *in vivo* evidence that MAST/Orbit is required during prometaphase for spindle elongation and becomes essential for spindle stabilization during the metaphase-anaphase transition.

Cell cycle progression after MAST RNAi

To analyze the immediate effects of MAST ablation on cell cycle progression, we performed dsRNAi in *Drosophila* S2 cells. Immunoblotting analysis showed that MAST levels decreased significantly within the first 48 h after the addition of dsRNA and the protein was barely detectable by 144 h (Fig. 3 A, left). Serial dilution experiments enabled us to deter-

Figure 2. In vivo analysis of mitotic progression in early *mast*⁵ embryos. Control and *mast*⁵ embryos carrying the *gfp-polo* transgene were followed by confocal time-lapse microscopy. (A) Time-lapse series of GFP-Polo fluorescence images showing the organization of the mitotic apparatus during mitotic progression in control *gfp-polo* (left) and *gfp-polo; mast*⁵ (right) embryos during cycle 12. Time is shown in seconds. Arrowheads represent the positioning of centrosomes in two sample nuclei. For discussion see text. (B) Graphic representation of kinetochore distribution on the spindle of wild type and *mast*⁵ at metaphase. The position of centrosomes is labeled as c. (C) Quantification of changes in spindle length in wild-type and *mast*⁵ embryos during mitosis. Measurements are from time-lapse confocal images taken every 10 s, taking the initiation of NEB as a reference point. The times corresponding to the images represented in A are indicated by an asterisk. Spindle length data correspond to the average measurement of seven nuclei in two different embryos (14 spindles in total). Error bars represent the standard deviation of the sample.



mine that addition of 10 $\mu\text{g/ml}$ of dsRNA to 10^6 exponentially growing S2 cells was sufficient to cause >90% reduction in the levels of MAST after 48 h (Fig. 3 A, right). To assess the effects of RNAi upon the cultured cells, samples were collected every 24 h and cell number, mitotic index, and cell viability were determined. Compared with the control population within the first 72 h, MAST RNAi caused a slight increase in the cell doubling time, from 23.6 to 27.5 h, however, between 72 and 144 h, the doubling time increased significantly, from 56.4 to 93.7 h (Fig. 3 B). By 72 h of RNAi, the mitotic index increased five- to sixfold (Fig. 3, C and F, and F'). Later, the mitotic index decreased, coincident with a slowing of the growth rate (Fig. 3, B, and C). RNAi did not affect cell viability significantly, as determined by trypan blue staining of dead cells (unpublished data).

To quantify the mitotic stages after MAST RNAi, we scored MAST-negative cells (identified by immunofluores-

cence) that were also immunostained to visualize α -tubulin (Fig. 3, D and D'; unpublished data). The results indicate that throughout the course of the RNAi experiment, most mitotic cells (>90%) were in a prometaphase-like stage, displaying either monopolar spindles or spindles that were bipolar with chromosomes that were not aligned at the metaphase plate. Our in vivo results in *mast*⁵ embryos revealed that the monopolar spindle formation is likely to occur after prometaphase. Consistently, after 48 h, no cells in metaphase, anaphase, or telophase were found (Fig. 3 D'). Instead, at much later times (120 h), cells in an anaphase-like (Fig. 3 D' and Fig. 4 E) or telophase-like configuration (Fig. 3 D' and Fig. 4 G), containing clustered centrosomes at only one pole, became more frequent.

After 72 h of exposure to MAST dsRNA, a significant proportion of the interphase cells had a single nucleus that was substantially larger than that of control cells (Fig. 3, E and

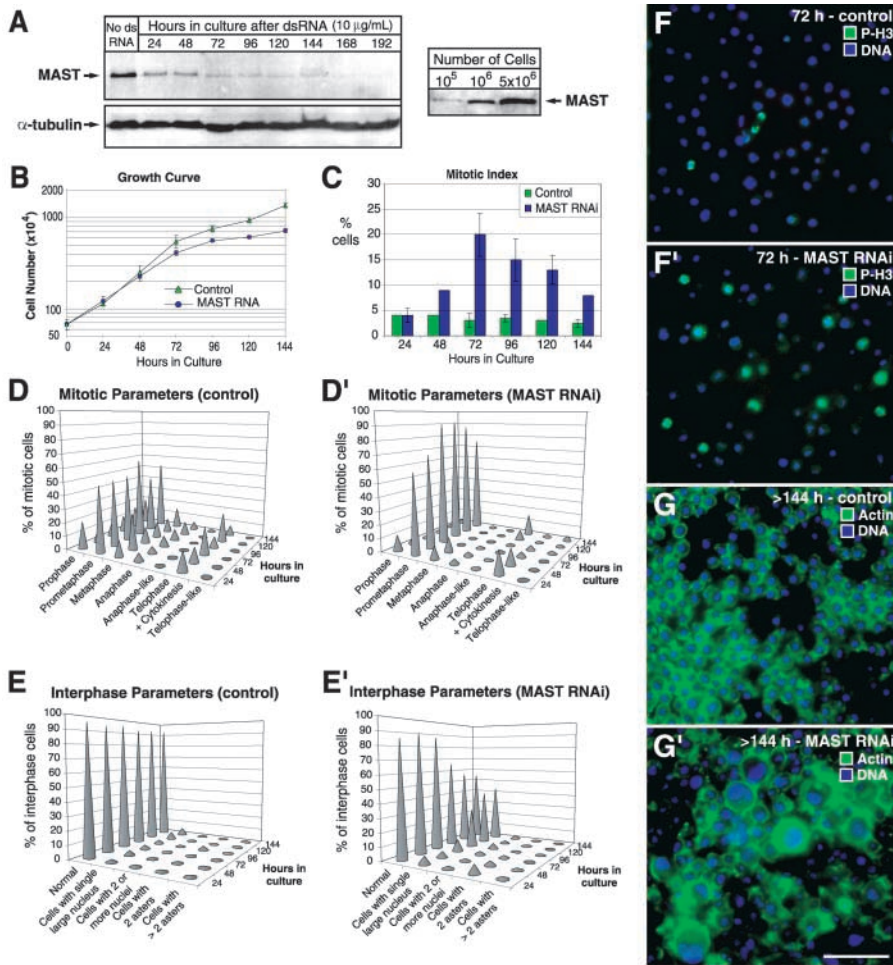


Figure 3. Time course analysis of MAST RNAi in *Drosophila* S2 cells. (A, left) MAST inactivation was monitored over time by Western blot analysis. 10⁶ cells were loaded in each lane and α -tubulin detection was used as a loading control. (A, right) Titration of anti-MAST antibody. (B) Proliferation analysis of S2 cells after MAST RNAi. (C) Mitotic index after MAST RNAi is represented as the average percentage of mitotic cells ($n > 100$) in the total population. (D and D') Quantification of the mitotic parameters during the course of the experiment in control and in cells after MAST RNAi, respectively ($n > 100$). (E and E') Quantification of interphase parameters during the course of the experiment in control and in cells after MAST RNAi ($n > 250$). (F and F') Low magnification views of representative optical fields by 72 h in control and MAST RNAi cells, respectively, stained with an anti-P-histone 3 antibody to detect cells undergoing mitosis or, after 144 h (G and G'), stained for actin. Note the formation of cells with a very large (four- to fivefold) nucleus after MAST RNAi. Bar, 50 μ m.

E'). Staining cells for actin and DNA indicated that after 144 h, MAST-depleted cells were up to fivefold larger in diameter when compared with control interphase cells (Fig. 3, G and G'). This indicates that after a long exposure to MAST RNAi, a significant proportion of cells becomes polyploid. A very similar phenotype was previously described for *mast*^d, a severe hypomorph allele (Lemos et al., 2000). The increase in ploidy and size of the MAST RNAi-treated cells does not appear to be due to prolonged mitotic arrest, because control cultures incubated for the same period in the presence of the microtubule poison colchicine arrest in mitosis, fail to show any significant increase in ploidy, and ultimately undergo massive apoptosis (unpublished data).

Organization of the mitotic apparatus in MAST RNAi-treated cells

To characterize the organization of the mitotic apparatus after MAST RNAi, cells were collected every 24 h and immunostained to visualize the spindle (α -tubulin), centrosomes (CP190), and chromosomes (DAPI) (Fig. 4). In most control cells, the mitotic apparatus was well organized with a single centrosome at each pole (Fig. 4, A and H). During the course of the experiment, between 5 and 10% of mitotic cells of both control and RNAi-treated S2 cells had asymmetric spindles with an irregular centrosome number at each pole (Fig. 4, H and H', bipolar asymmetric). However, after a

48-h exposure of cells to dsRNA, there was a large increase in the frequency of cells with monopolar spindles, and no cells in metaphase, anaphase, or telophase were found (Fig. 3 D'). This phenotype was maximal at 72 h (Fig. 4, B and H'). After 96 h, two different prometaphase-like cell populations were observed. About half appeared polyploid with a monopolar spindle surrounding a cluster of several centrosomes (≥ 4) (Fig. 4, C and H'). However, nearly 20% showed a bipolar array of microtubules with centrosomes at only one pole (Fig. 4, D and H', bipolar acentrosomal). Other cells adopted an anaphase-like configuration with a distinct set of chromosomes near each pole (Fig. 4, E-E''', and Fig. 3 D', after 120 h). At even later time points in the RNAi experiment (Fig. 3 D', 144 h), a small percentage of cells (3%) were in a telophase-like state with an organized central spindle structure and decondensed chromatin with no or very reduced immunostaining with antiphosphohistone H3 antibody (Fig. 4, G-G''; unpublished data). Interestingly, the centrosomes in these cells were found clustered at a single pole. Further characterization of these abnormal forms of mitotic exit is currently under study (unpublished data).

Characterization of chromosome behavior after MAST RNAi

To determine whether sister chromatids had separated in MAST-depleted cells, we performed immunofluorescence anal-

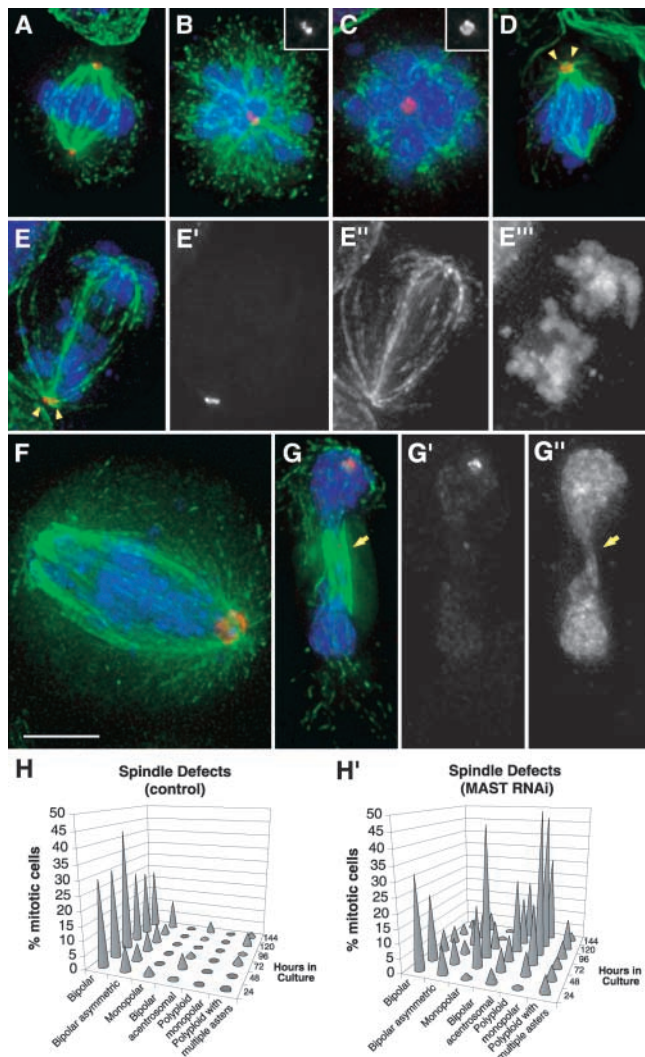


Figure 4. Organization of the mitotic apparatus after MAST RNAi. Cells after MAST RNAi were stained with an anti-CP190 antibody to reveal the centrosomes (red), an anti- α -tubulin antibody to visualize the microtubules (green), and DAPI to counterstain the DNA (blue). (A) Normal bipolar spindle in a control cell. (B and C) Monopolar and polytropic monopolar spindles with two and at least four centrosomes, respectively, observed 72 or 96 h after MAST RNAi. Centrosome staining alone can be seen in the insertion on top right of the figures. (D) Bipolar spindle with two centrosomes (arrowheads) only in one pole. (E) Anaphase-like cell displaying a bipolar spindle with centrosomes in a single pole and chromosomes distributed in two distinct populations on each side of the spindle. Unmerged images revealing the centrosomes (E'), spindle (E''), and chromosomes (E''') are shown. (F) A cell with a bipolar spindle and multiple centrosomes clustered in a single pole where the chromosomes appear distributed along the spindle. (G) Abnormal telophase-like cell showing the formation of a cleavage furrow (arrows), with centrosomes in only one pole and decondensed chromatin. Separate centrosome and DNA staining can be seen in (G') and (G''), respectively. (H and H') Quantification of the observed spindle defects in control and MAST-depleted cells, respectively ($n > 100$).

ysis to localize the kinetochore markers BubR1 (unpublished data) and Cid, the *Drosophila* CENP-A homologue (Henikoff et al., 2000). In control cells (Fig. 5 A), BubR1 staining on kinetochores was maximal during prometaphase. As cells pro-

gressed into metaphase and the chromosomes aligned at the metaphase plate, BubR1 intensity decreased and was barely detected after anaphase onset (Fig. 5, A and C). After RNAi, BubR1 was localized on kinetochores of anaphase-like cells (Fig. 5, B–B'') as well as in cells with monopolar spindles (Fig. 5, D and D'). BubR1 was present on all chromosomes and stained kinetochore pairs almost as intensively as in control prometaphase cells, clearly indicating that sister chromatids did not disjoin before migrating to the poles (Fig. 5, B–C; unpublished data). Identical results were obtained when either anaphase-like or monopolar cells were stained with anti-Cid antibodies (Fig. 5, E–E'', and Fig. 6). These results indicate that chromosomes failed to undergo sister chromatid separation even in cells that displayed an anaphase-like configuration.

Characterization of microtubule–kinetochore attachment after MAST RNAi

To determine whether spindle microtubules in MAST-depleted cells are able to establish stable end-on interactions with kinetochores, RNAi-treated cells were immunostained for tubulin and the kinetochore marker Cid, with or without a preincubation in a buffer containing calcium, to selectively dissociate nonkinetochore microtubules (Mitchison et al., 1986; Kapoor et al., 2000), or taxol, to promote microtubule stabilization (Fig. 6). Consistent with published observations, in the presence of calcium, most kinetochores were clearly seen to associate specifically with the ends of microtubule bundles (Fig. 6, A–B'). However, in MAST-depleted bipolar prometaphase cells, kinetochores were distributed along the spindle (Fig. 6, C–D') and never organized a metaphase plate. In MAST-depleted cells with monopolar spindles, chromosomes were mostly buried within the aster, and kinetochores either did not associate with the plus ends of microtubules or appear to bind short microtubules (Fig. 6, E–F' and I). However, if RNAi-treated cells were incubated for 30 min with taxol, 75% of kinetochore pairs were associated with the plus ends of long microtubule bundles (Fig. 6, G–H'). Furthermore, the distribution of chromosomes relative to the aster was significantly different in the presence of taxol, with chromosomes localized at the periphery and most kinetochores facing the center (Fig. 6, compare E–F' with G–H'). These data show that if microtubule dynamics are suppressed in MAST-depleted cells, long microtubule bundles are formed with kinetochores associated at their plus ends.

Ultrastructural analysis of MAST-depleted S2 cells

To analyze in more detail the organization of the mitotic apparatus and the attachment of chromosomes to the spindle after depletion of MAST, RNAi-treated cells were processed for transmission electron microscopy (Fig. 7). In control mitotic cells, we could observe bipolar spindles organized from well-defined centrosomes (Fig. 7, A and A2). In these cells, bundles of microtubules were visible running from the spindle pole and making contact with individual chromosomes at the kinetochore (Fig. 7, A1 and A1'). However, in MAST-depleted cells that showed a monopolar organization (Fig. 7, B and C), we found no evidence of microtubule bundling, and chromosomes were located close to the center of the aster where multiple centrioles could be found (Fig. 7 B). A higher mag-

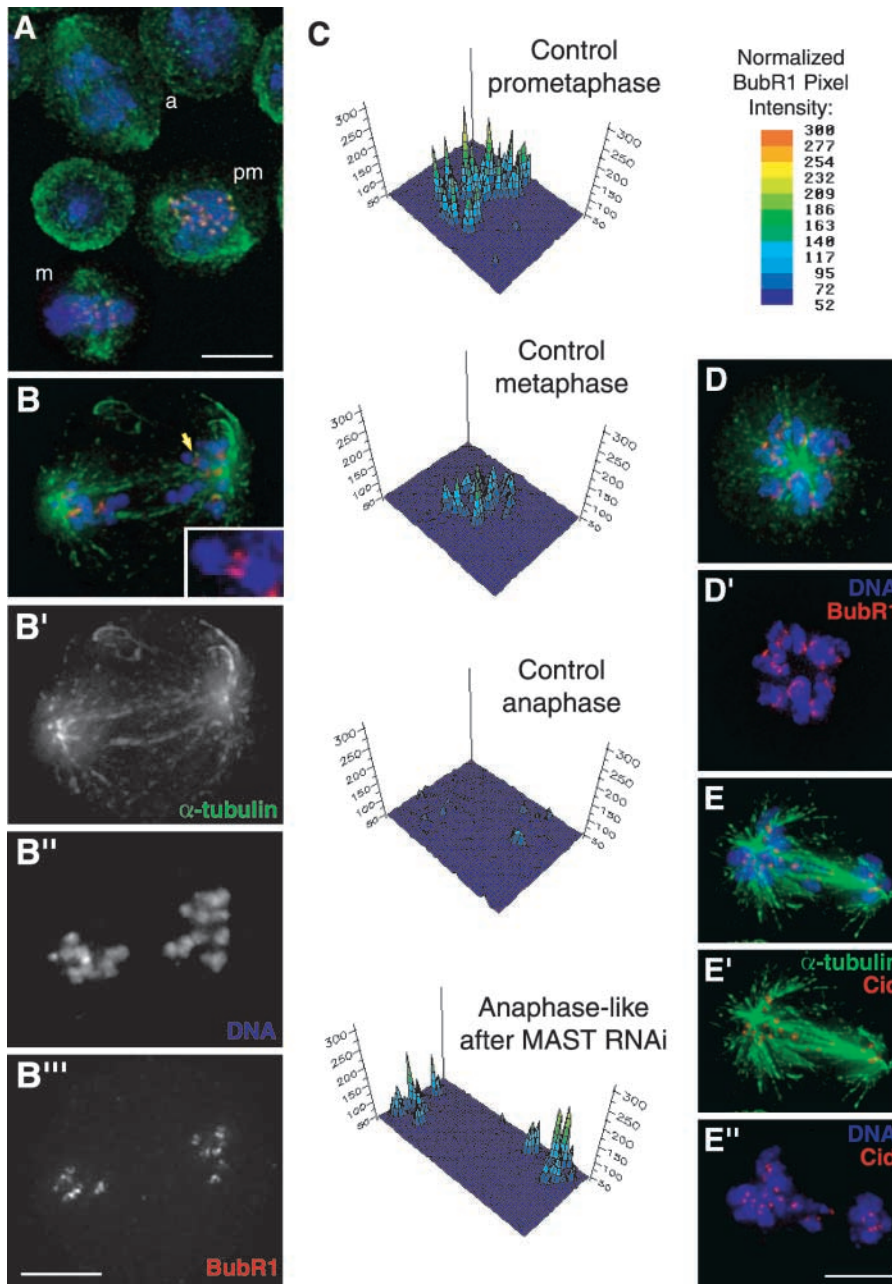


Figure 5. Sister chromatid separation in cells after MAST RNAi. (A–C) Samples were collected between 96 and 144 h after MAST RNAi and processed for immunofluorescence analysis with anti-BubR1 and anti-Cid antibodies as markers for kinetochores (red). Microtubules were stained with an anti- α -tubulin antibody (green), and chromosomes were counterstained with DAPI (blue). (A) Control cells in the same optical field undergoing prometaphase (pm), metaphase (m), and anaphase (a).

(B) Anaphase-like cells after MAST RNAi showing very strong BubR1 staining at both kinetochores of each chromosome (arrow; 3 \times amplified insert), confirming that sister chromatid separation has not taken place. Unmerged images showing the mitotic spindle (B'), chromosomes (B''), and BubR1 (B''') can be seen separately. (C) Quantification of normalized BubR1 pixel intensity in the control cells shown in A and the anaphase-like cell shown in B. (D and D') Cell after MAST RNAi, showing the monopolar spindle organization with very strong BubR1 staining at kinetochore pairs. (E–E') Cid staining on anaphase-like cells revealed that >90% of these cells ($n = 20$) show an unequal number of chromosomes in each pole that seem to interact laterally with the spindle microtubules. Bars, 5 μ m.

nification view of a cell with a monopolar spindle shows chromosomes on the same plane of individual microtubules, suggesting that lateral interactions take place (Fig. 7 C). These results are consistent and further support the observations that depletion of MAST/Orbit perturbs the interaction between kinetochores and the plus ends of spindle microtubules.

Distribution of ZW10, dynein, and D-CLIP-190 in the absence of MAST

To further ascertain whether the interactions between kinetochores and microtubules are altered after MAST RNAi, we analyzed the distribution of ZW10 and dynein, two proteins that localize to kinetochores early in mitosis and are transferred to spindle microtubules after kinetochore attachment (Williams et al., 1992; King et al., 2000). The results show that in control cells (Fig. 8, A–B'), ZW10 was local-

ized to kinetochores of mono-oriented chromosomes during prometaphase and extended along the spindle microtubules at metaphase, whereas, after RNAi treatment, it was always found associated with the kinetochores in cells with both monopolar and bipolar spindles (Fig. 8, C–D'). Similarly, in control cells, dynein showed accumulation in kinetochores of mono-oriented chromosomes during prometaphase (Fig. 8 E) and there was little or no staining at metaphase (Fig. 8 F), whereas, in RNAi-treated cells, dynein was always found associated with kinetochores (Fig. 8, G and G'). We have also analyzed the distribution of D-CLIP-190 (Lantz and Miller, 1998), the *Drosophila* homologue of CLIP-170, a protein that has been shown to bind CLASPs (Akhmanova et al., 2001), the human homologues of MAST. D-CLIP-190 was found associated with kinetochores of prometaphase chromosomes (Fig. 8, H and H'), but at metaphase,

Figure 6. Analysis of kinetochore–microtubule attachment in MAST-depleted cells. Control cells (A–B') as well as MAST-depleted cells by RNAi (C–H') were stained with antibodies against Cid (red) and α -tubulin (green) and counterstained with DAPI to reveal the DNA (blue). (A and A') Control cell in metaphase showing that all the kinetochores are end-on attached to microtubules. (B and B') Control cell in metaphase that was pretreated with calcium before fixation, showing that the kinetochore microtubules were selectively preserved. (C–D') Cells with bipolar spindles after MAST RNAi with misaligned chromosomes without (C and C') or with (D and D') a pretreatment with calcium. (E–E' and F–F') Cells with monopolar spindles after MAST RNAi with or without a pretreatment with calcium, respectively, showing chromosomes buried close to the center of the aster, and the kinetochores cannot be found associated with microtubule plus ends. (G–H') Treatment of MAST-depleted cells with taxol leads chromosomes to be organized at the periphery of the aster clearly associated with microtubule plus ends. Insertions inside panels represent the selected area in the cells that was magnified twice. Bars, 5 μ m.

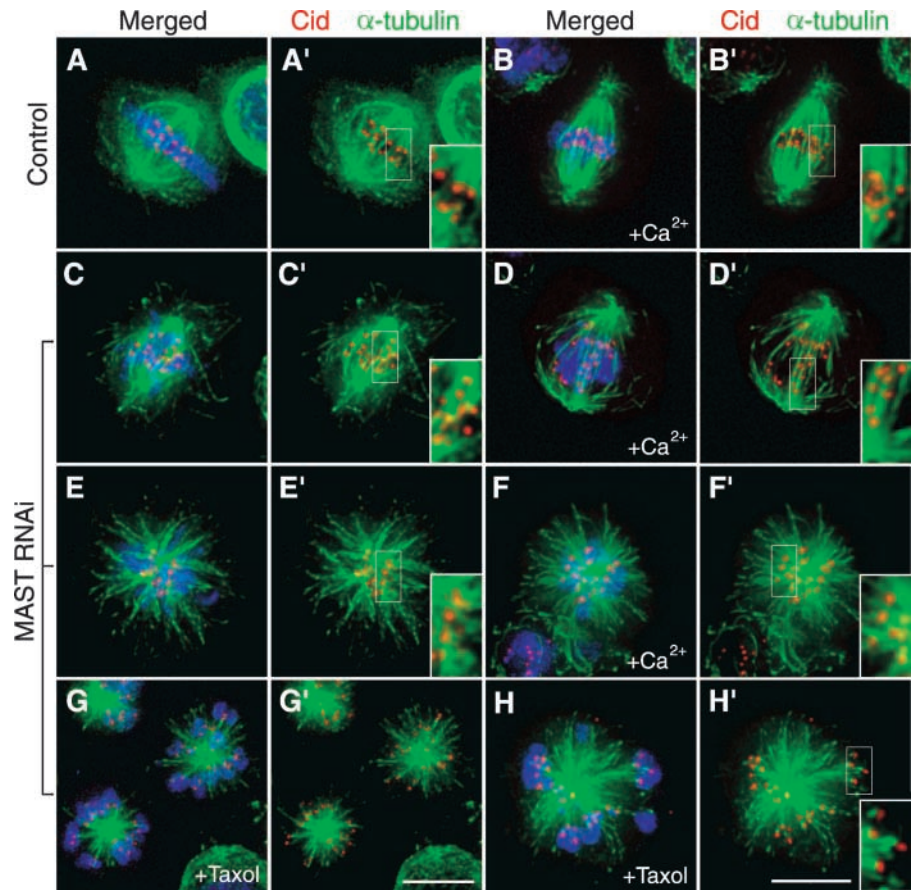
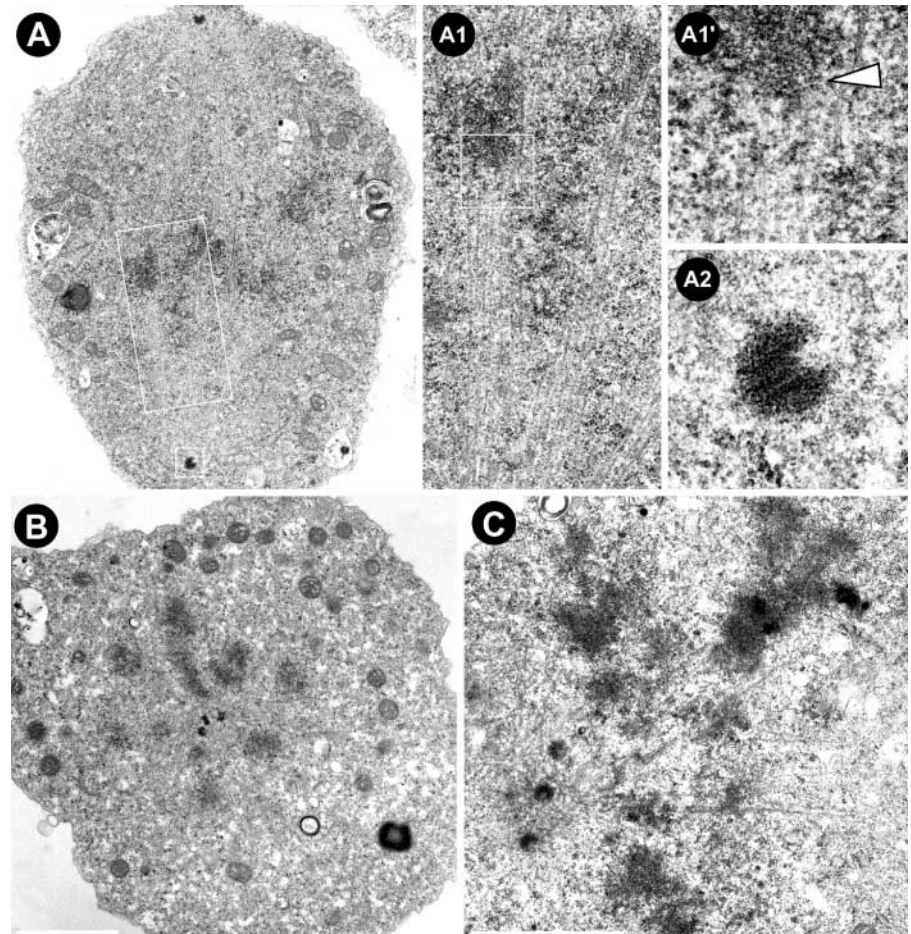


Figure 7. Ultrastructural analysis of S2 cells after MAST RNAi. (A) Control cell showing a bipolar spindle with bundles of microtubules organized from the centrosomes. (A1) Higher magnification of chromosomes being captured by bundles of microtubules in a region that corresponds to the kinetochore (A1', arrowhead). (A2) Higher magnification of one of the centrosomes. (B) Top view of a MAST-depleted cell after RNAi showing a monopolar spindle with chromosomes very close to the center of the aster where three centrosomes can be seen. (C) Side view of another MAST-depleted cell showing a monopolar aster where individual microtubules can be seen on the same plane of the chromosomes, suggesting lateral interactions. Bars, 2 μ m.



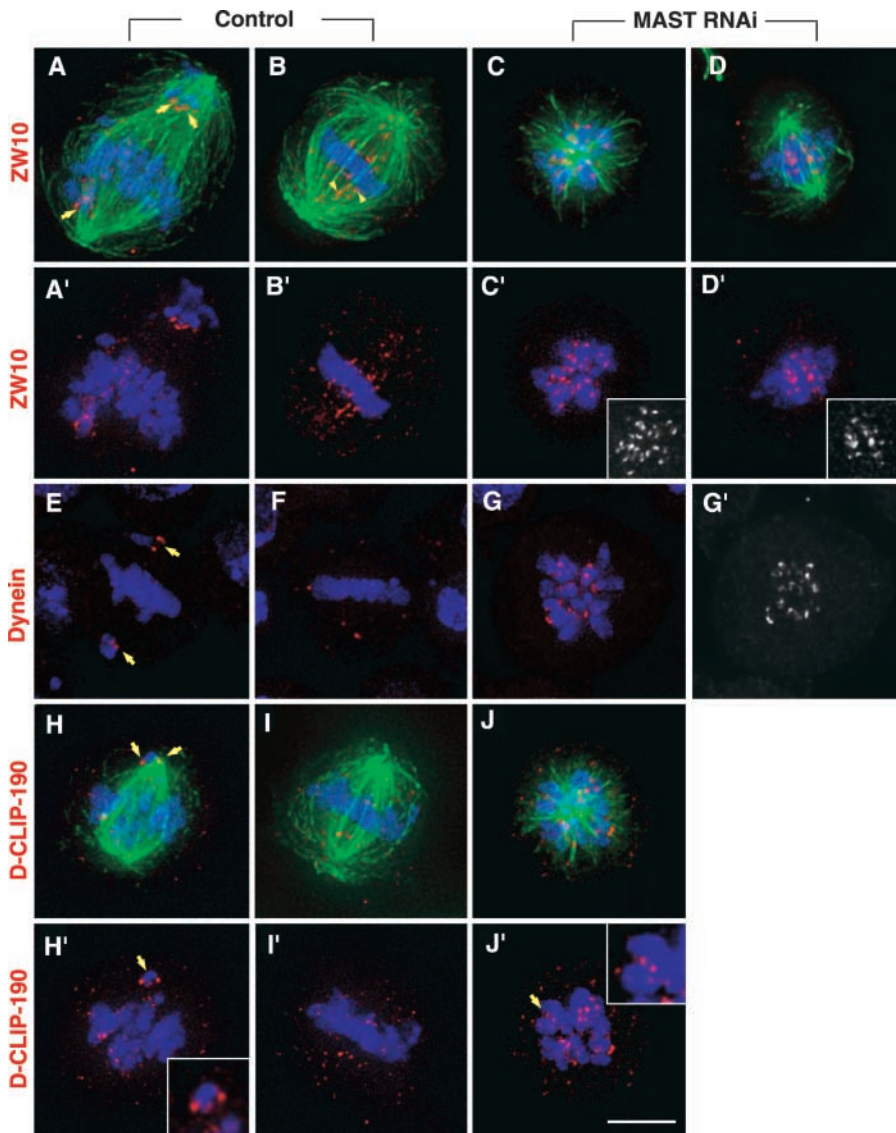


Figure 8. Immunolocalization of kinetochore-associated proteins in the absence of MAST. (A–B', E, F, and H–I') Untreated control cells or (C–D', G, G', J, and J') cells 72 h after MAST RNAi, were stained (red) with anti-ZW10, anti-dynein, and anti-D-CLIP-190 antibodies. α -Tubulin (green) and DNA (blue) are also shown when possible. (A, A', E, H, and H') Cells in prometaphase with mono-oriented chromosomes showing kinetochore-associated ZW10, dynein, and D-CLIP-190 (arrows). (B, B', F, I, and I') During metaphase, when all the chromosomes become bioriented, ZW10 transfers to the kinetochore microtubules (arrowheads), and dynein and D-CLIP-190 are barely detectable at the kinetochores. (C and C') Cells with monopolar or (D and D') bipolar spindles with misaligned chromosomes showing strong staining of ZW10 at kinetochores. Insertions in panels C' and D' show ZW10 staining alone. In cells with monopolar spindles, after MAST RNAi, dynein (G and G') and D-CLIP-190 (J and J') show strong accumulation at kinetochores. Insertions in panels H' and J' show magnified views of the chromosomes indicated by the arrows. Bar, 5 μ m.

we found the staining dispersed over the spindle region (Fig. 8, I and I'). After RNAi, monopolar cells showed D-CLIP-190 staining mostly associated with kinetochore pairs, although some punctate staining was also visible in the area of microtubules (Fig. 8, J and J'). These results show that after depletion of MAST, ZW10 and dynein were retained at the kinetochores. Furthermore, the data also show that the kinetochore localization of D-CLIP-190 was not dependent upon the presence of MAST/Orbit.

Discussion

Possible roles for MAST/Orbit in microtubule–kinetochore attachment

The studies reported here provide strong evidence suggesting that MAST/Orbit is required for microtubule plus ends to establish a functional attachment to kinetochores. In the absence of MAST/Orbit, chromosome congression does not take place and kinetochores either do not show a clear end-on attachment or appear to bind through lateral interactions. Most surprising is the monopolar configuration in MAST-

depleted cells where we find chromosomes mostly localized close to the center of the aster. If, in MAST-depleted cells, the microtubule–kinetochore interaction is compromised, it would be expected that the action of chromokinesins and even passive impacts by elongating microtubules would push the chromosomes to the periphery of the asters (the “polar wind”). This suggests that the localization of chromosomes to the interior of asters is likely to involve an active, rather than a passive, process that can be explained by at least three different models. MAST/Orbit could be required for kinetochores to hold on to dynamic microtubules. If it were true that in cells lacking MAST/Orbit, kinetochores could not hold onto shortening microtubules, then every time a kinetochore fiber would begin to shorten, it would be released by its kinetochore. That kinetochore would then have to make an initial encounter with microtubules all over again through lateral interactions that could be mediated by cytoplasmic dynein, as it is during prometaphase, and the chromosome would be expected to exhibit rapid poleward movement (Rieder et al., 1990). Consistent with this model, levels of kinetochore-associated dynein and ZW10 remained abnormally elevated in

the absence of MAST. A second interpretation of these results is that in the absence of MAST/Orbit, chromosomes attach to microtubules that can shorten but cannot regrow so that chromosomes would end up mostly in the region close to the center of the aster, suggesting that MAST/Orbit could have a role in promoting microtubule plus end stability. Indeed, the human homologues, CLASPs, have been shown to promote plus end microtubule stabilization in interphase (Akhmanova et al., 2001). However, MAST/Orbit does not appear to affect the ability of all microtubules to elongate, because in MAST-depleted cells, there is no obvious effect upon growth of astral microtubules. Therefore, if MAST/Orbit has a role in microtubule dynamics, kinetochore microtubules are particularly sensitive. Finally, it is also possible that in MAST-depleted cells, kinetochores attach to microtubules, but minus end-directed motility of the kinetochore dominates so that the movement of chromosomes toward the poles prevails over the polar wind, pushing the chromosomes toward the plus ends of microtubules. It could be that kinetochore-associated MAST (Lemos et al., 2000) is required for the binding of essential kinesins with plus end-directed motility. A putative candidate could be CENP-E, a plus end-directed motor (Wood et al., 1997) that has been shown to localize to the fibrous corona of the kinetochore (Cooke et al., 1997) and be required for stable, bioriented attachment of chromosomes to spindle microtubules (Yao et al., 2000). Surprisingly, depletion of CENP-E by microinjection also causes misaligned chromosomes to be sequestered very close to the spindle poles (McEwen et al., 2001).

Although, at present, the data presented here does not allow us to clearly distinguish amongst these interpretations, we favor the first two models because they could readily explain the results obtained after taxol treatment of MAST-depleted cells. Suppressing microtubule dynamics after depletion of MAST/Orbit causes the formation of monopolar cells, with most kinetochores associated to the plus ends of microtubule bundles. MAST/Orbit could be part of a protein complex required to hold on to the plus ends of dynamic microtubules. Alternatively, MAST/Orbit could be required for microtubule plus end stabilization. Thus, in the absence of MAST/Orbit, kinetochores attach to microtubules, and facilitating their stabilization could allow the formation of a kinetochore fiber and its growth. Consistent with this interpretation, it has been shown that the fission yeast orthologue of CLIP-170, tip1p, is an anticatastrophe factor (Brunner and Nurse, 2000). Thus, it is possible that the defects we observed after loss or mutation of MAST could be due to an effect on D-CLIP-190 (the *Drosophila* homologue of mammalian CLIP-170). However, we have shown here that the localization of D-CLIP-190 to kinetochores is normal in the absence of MAST. Nevertheless, we cannot exclude that MAST could have a dual role affecting both kinetochore attachment and microtubule stability, as has been recently described for Bik1, the budding yeast homologue of CLIP-170 (Lin et al., 2001).

MAST function is required to maintain spindle bipolarity

In vivo analysis of *mast*⁵ mutant embryos demonstrates that MAST becomes essential for the maintenance of a bipolar spindle during metaphase; in its absence, the spindle col-

lapses and centrosomes slide toward the metaphase plate forming monopolar spindles. STU1p, the putative MAST orthologue in *S. cerevisiae*, is also essential for spindle stability (Pasqualone and Huffaker, 1994). It is now well accepted that a balance between plus end- and minus end-directed motors is essential for the maintenance of a bipolar spindle through metaphase and also for its elongation during anaphase (Sharp et al., 2000a). This has been best studied in *S. cerevisiae*, where imbalances between the Cin8p/Kip1p and Kar3p kinesins cause rapid collapse of the bipolar spindle (Saunders and Hoyt, 1992). Thus, it is possible that MAST is required for the stable association of one or more kinesins with the microtubules and that in the absence of this kinesin, the balance of power is perturbed at metaphase. Indeed, the collapse of the spindle seen after depletion of MAST is very similar to the effect caused by depletion of the *Drosophila* bipolar kinesin-like KLP61F (Heck et al., 1993, Sharp et al., 2000a). The presence of MAST in the midzone (Lemos et al., 2000) suggests that MAST may also be acting by cross-linking interpolar microtubules and so stabilizing the spindle. It is also possible that depletion of MAST perturbs the distribution or function of other MAPs that are required for formation of a functional bipolar spindle. These could include the chromosomal passengers INCENP and aurora-B (Adams et al., 2001; Giet and Glover, 2001). In fact, we did observe aberrant behavior of these proteins in anaphase-like cells after depletion of MAST by dsRNAi (unpublished data).

MAST-depleted cells show abnormal mitotic exit

Although depletion of MAST function by dsRNAi causes most cells to arrest in mitosis with monopolar spindles, after long incubation periods, a proportion of cells is seen to adopt an anaphase-like configuration with paired sister chromatids migrating to the poles. These cells are cyclin B positive (unpublished data), retain BubR1 at the kinetochores, and also appear to undergo cytokinesis with an actin contractile ring (unpublished data). A large proportion of these cells progress into further cycles of DNA replication and become polyploid. Because S2 cells have a functional spindle checkpoint, as shown by their ability to arrest in mitosis in the presence of colchicine and also by their initial accumulation in mitosis after MAST depletion, we believe it is likely that MAST-depleted cells bypass the checkpoint and exit mitosis. Further characterization of this abnormal mitotic exit in MAST-depleted cells is currently underway, and the results will be published elsewhere (unpublished data).

Materials and methods

DsRNAi in *Drosophila* S2 cells

For MAST RNAi in *Drosophila* S2 cells, we synthesized a fragment of ~700 bp of dsRNA corresponding to the 5' region of *mast* cDNA covering the ATG encoding the first methionine as previously described (Clemens et al., 2000), except that 10 µg of dsRNA per ml of culture medium was used. Treatment of S2 cells with dsRNA synthesized from random human intronic sequence, to rule out unspecific effects of dsRNA, caused no visible defects and was indistinguishable from the untreated control.

Cell culture, immunofluorescence, and Western blot analysis

For immunofluorescence, cells were grown and processed as previously described (Adams et al., 2001), except for those that were pretreated with calcium (Kapoor et al., 2000). Anti-MAST antibody and Western blot analysis were described previously (Lemos et al., 2000). Other antibodies used

were mouse or rabbit anti-CP190 (Whitfield et al., 1988); mouse anti- α -tubulin and anti- γ -tubulin (Sigma-Aldrich); rabbit or mouse anti-phosphorylated-H3 (Upstate Biotechnology and New England Biolabs, Inc.); rabbit anti-Cid (Henikoff et al., 2000); rabbit anti-BubR1 (C. Lopes and H. Bousbaa, University of Porto); rabbit anti-ZW10 (Williams et al., 1992); mouse anti-dynein (McGrail and Hays, 1997); and affinity-purified rabbit anti-D-CLIP-190 (Lantz and Miller, 1998). FITC-phalloidin (Molecular Probes) was used to detect actin. Secondary antibodies for immunofluorescence were FITC- α -rabbit or Texas red- α -mouse (Jackson ImmunoResearch Laboratories). Quantitative three-dimensional datasets of representative cells were collected using a DeltaVision microscope (Applied Precision), based on an Olympus IX-70 inverted microscope with a Photometrics CH350L cooled CCD camera, and subsequently deconvolved and projected onto a single plane using SoftWorx (Applied Precision), except for low magnification images shown in Fig. 3. Adobe Photoshop® 5.5 (Adobe Systems, Inc.) was used to process all images.

Transmission electron microscopy

Control and MAST-depleted cells were collected 72 h after RNAi and embedded for sectioning as described previously (Rieder and Cassels, 1999), with the exception that Agar 100 resin was used. Serial sections were cut on a Leica Ultracut UCT ultramicrotome and collected on 100 mesh copper grids. Sectioned cells were stained with 4% aqueous uranyl acetate for 1 h in the dark and then left for 10 min in lead citrate in a CO₂-free atmosphere. Samples were observed with a Philips CM 120 Biotwin using Eastman Kodak Co. SO 163 electron image film.

Scoring of MAST RNAi phenotype

The growth curves were plotted considering only viable cells stained with Trypan blue (Sigma-Aldrich), and doubling time was calculated from the equations corresponding to the best fit. Mitotic index was determined as the percentage of mitotic cells in the total population. Only MAST-negative cells were scored for mitotic parameters in the RNAi experiments. Spindle defects were scored as a percentage of mitotic cells and were confirmed independently in three distinct experiments either by γ -tubulin or CP190 staining in MAST-negative cells. Quantification of microtubule-kinetochore attachment was performed by detection of Cid, used as a kinetochore marker, at the tips of microtubules in five distinct monopolar cells. Taxol was used at 10 μ M during the 30 min before fixation to allow for the stabilization of spindle microtubules.

Mobilization of the P element in *mast*¹ and generation of *mast*⁵

The *mast*⁵ allele was obtained from the same P element mobilization program described previously (Lemos et al., 2000), and molecular characterization was done by Southern blot analysis. *mast*⁵ homozygous females lay eggs that die during embryogenesis when crossed to either *mast*⁵ or wild-type males. Complementation analysis with other *mast* mutant alleles, including *orbit*¹, or a deletion (Df(3L) 31A) that uncovers the *mast* region results in a similar mutant phenotype to that observed in homozygous *mast*⁵ embryos.

Immunofluorescence in embryos

The embryos were prepared for immunostaining as previously described (González and Glover, 1993). Immunostaining of microtubules and centrosomes was performed with antibodies against α -tubulin (Amersham Pharmacia Biotech) and centrosomin (Heuer et al., 1995). Primary antibodies were detected with FITC- α -mouse (Vector Laboratories) or CY3- α -rabbit (Jackson ImmunoResearch Laboratories) conjugated immunoglobulins. The preparations were visualized in a ZEISS Axioskop microscope, and images were acquired with a SPOT2 camera (Diagnostic Instruments) and processed with Adobe Photoshop® 5.5.

Live analysis of *gfp-polo*; *mast*⁵ embryos

The *gfp-polo* transgene was introduced in the *mast*⁵ strain to obtain the strain *w*; *P[gfp-polo]*; *mast*⁵/TM6B. *gfp-polo*; *mast*⁵ embryos were hand dechorionated and mounted in oil holocarbon 700 (Sigma-Aldrich). Images were collected with a Bio-Rad Laboratories MRC600 confocal microscope at 10-s intervals using Comos software (Bio-Rad Laboratories). Image stack processing and animation, as well as measurement of spindle length, were done with ImageJ (<http://rsb.info.nih.gov/ij/>). Quantification of chromosome congression was performed by determining the relative coordinates of the kinetochore GFP-Polo signal relative to two imaginary axes, one running between the center of the centrosomes and the other drawn perpendicular to the first at the midpoint. To compare measurements from different dividing nuclei, the centrosome-to-centrosome length was normalized to two arbitrary units. A total of 132 kinetochore pairs from 20 dividing nuclei of two separate experiments were scored.

Online supplemental material

Quicktime™ videos associated with Fig. 2 are provided as supplemental material and can be viewed at <http://www.jcb.org/cgi/content/full/jcb.200201101/DC1>. The movies show the organization of the mitotic apparatus visualized by GFP-Polo during mitotic progression in control *gfp-polo* (Video 1) and mutant *gfp-polo*; *mast*⁵ (Video 2) embryos during cycle 12.

We would like to thank C. Rieder and G. Cassels (Wadsworth Center for Laboratories and Research, Albany, NY) for protocols and EM advice; C. Lopes, H. Bousbaa, and M. Costa for allowing the use of unpublished reagents; and A. Merdes, C. Morrison, K. Sawin, S. Wheatley, and M. Heck (Wellcome Institute for Molecular Biology) for discussions and critical reading of the manuscript. We are also indebted to M. Heck for sharing valuable reagents. We thank all the members of the C.E. Sunkel and W.C. Earnshaw laboratories for suggestions and encouragement.

H. Maiato is supported by the Gulbenkian PhD Programme in Biology and Medicine. P. Sampaio has a post-doctoral fellowship and C.L. Lemos has a PhD studentship both supported by PRAXIS XXI of Fundação para a Ciência e a Tecnologia. The work in the W.C. Earnshaw laboratory is financed by the Wellcome Trust, of which he is a Principal Research Fellow. FCT and the TMR Program of the EU finance work in C.E. Sunkel laboratory.

Submitted: 23 January 2002

Revised: 28 March 2002

Accepted: 9 April 2002

References

- Adams, R.R., H. Maiato, W.C. Earnshaw, and M. Carmena. 2001. Essential roles of *Drosophila* inner centromere protein (INCENP) and aurora B in histone H3 phosphorylation, metaphase chromosome alignment, kinetochore disjunction, and chromosome segregation. *J. Cell Biol.* 153:865–879.
- Akhmanova, A., C.C. Hoogenraad, K. Drabek, T. Stepanova, B. Dortland, T. Verkerk, W. Vermeulen, B.M. Burgering, C.I. De Zeeuw, F. Grosveld, and N. Galjart. 2001. CLSPs are CLIP-115 and -170 associating proteins involved in the regional regulation of microtubule dynamics in motile fibroblasts. *Cell.* 104:923–935.
- Brunner, D., and P. Nurse. 2000. CLIP170-like tip1p spatially organizes microtubular dynamics in fission yeast. *Cell.* 102:695–704.
- Clemens, J.C., C.A. Worby, N. Simonson-Leff, M. Muda, T. Machama, B.A. Hemmings, and J.E. Dixon. 2000. Use of double-stranded RNA interference in *Drosophila* cell lines to dissect signal transduction pathways. *Proc. Natl. Acad. Sci. USA.* 97:6499–6503.
- Cooke, C.A., B. Schaar, T.J. Yen, and W.C. Earnshaw. 1997. Localization of CENP-E in the fibrous corona and outer plate of mammalian kinetochores from prometaphase through anaphase. *Chromosoma.* 106:446–455.
- Dujardin, D., U.I. Wacker, A. Moreau, T.A. Schroer, J.E. Rickard, and J.R. De Mey. 1998. Evidence for a role of CLIP-170 in the establishment of metaphase chromosome alignment. *J. Cell Biol.* 141:849–862.
- Garcia, M.A., L. Vardy, N. Koonruga, and T. Toda. 2001. Fission yeast ch-TOG/XMAP215 homologue Alp14 connect mitotic spindles with the kinetochore and is a component of the Mad2-dependent spindle checkpoint. *EMBO J.* 20:3389–3401.
- Giet, R., and D.M. Glover. 2001. *Drosophila* aurora B kinase is required for histone H3 phosphorylation and condensin recruitment during chromosome condensation and to organize the central spindle during cytokinesis. *J. Cell Biol.* 152:669–681.
- Goh, P.-Y., and J.V. Kilmartin. 1993. *NDC10*: a gene involved in chromosome segregation in *Saccharomyces cerevisiae*. *J. Cell Biol.* 121:503–512.
- González, C., and D.M. Glover. 1993. Techniques for studying mitosis in *Drosophila*. In *The Cell Cycle: A Practical Approach*. P. Fantes and R. Brookes, editors. Oxford University Press, Oxford, UK. 163–168.
- He, X., D.R. Rines, C.W. Espelin, and P.K. Sorger. 2001. Molecular analysis of kinetochore-microtubule attachment in budding yeast. *Cell.* 106:195–206.
- Heck, M., A. Pereira, P. Pesavento, Y. Yannoni, and A.C. Spradling. 1993. The kinesin-like protein KLP61F is essential for mitosis in *Drosophila*. *J. Cell Biol.* 123:665–679.
- Henikoff, S., K. Ahmad, J.S. Platero, and B. van Steensel. 2000. Heterochromatic deposition of centromeric histone H3-like proteins. *Proc. Natl. Acad. Sci. USA.* 97:716–721.
- Heuer, J., K. Li, and T. Kaufman. 1995. The *Drosophila* homeotic target gene centrosomin (*cnn*) encodes a novel centrosomal protein with leucine zippers and maps to a genomic region required for midgut morphogenesis. *Develop-*

- ment. 121:3861–3876.
- Hoyt, M.A., and J.R. Geiser. 1996. Genetic analysis of the mitotic spindle. *Annu. Rev. Genet.* 30:7–33.
- Inoue, Y.H., M. do Carmo Avides, M. Shiraki, P. Deak, M. Yamaguchi, Y. Nishimoto, A. Matsukage, and D.M. Glover. 2000. Orbit, a novel microtubule-associated protein essential for mitosis in *Drosophila melanogaster*. *J. Cell Biol.* 149:153–165.
- Kapoor, T.M., T.U. Mayer, M.L. Coughlin, and T.J. Mitchison. 2000. Probing spindle-assembly mechanisms with monastrol, a small molecule inhibitor of the mitotic kinesin Eg5. *J. Cell Biol.* 150:975–988.
- King, J.M., T.S. Hays, and R.B. Nicklas. 2000. Dynein is transient kinetochore component whose binding is regulated by microtubule attachment, not tension. *J. Cell Biol.* 151:739–748.
- Lantz, V.A., and K.G. Miller. 1998. A class VI unconventional myosin is associated with a homologue of a microtubule-binding protein, cytoplasmic linker protein-170, in neurons and at the posterior pole of *Drosophila* embryos. *J. Cell Biol.* 140:897–910.
- Lemos, C.L., P. Sampaio, H. Maiato, M. Costa, L.V. Omel'yanchuk, V. Liberal, and C.E. Sunkel. 2000. MAST, a conserved microtubule-associated protein required for bipolar mitotic spindle organization. *EMBO J.* 19:3668–3682.
- Lin, H., P. de Carvalho, D. Kho, C.Y. Tai, P. Pierre, G.R. Fink, and D. Pellman. 2001. Polyploids require Bik1 for kinetochore–microtubule attachment. *J. Cell Biol.* 155:1173–1184.
- McEwen, B.F., G.K. Chan, B. Zubrowski, M.S. Savoian, M.T. Sauer, and T.J. Yen. 2001. CENP-E is essential for reliable bioriented spindle attachment, but chromosome alignment can be achieved via redundant mechanisms in mammalian cells. *Mol. Biol. Cell.* 12:2776–2789.
- McGrail, M., and T.S. Hays. 1997. The microtubule motor cytoplasmic dynein is required for spindle orientation during germline cell divisions and oocyte differentiation in *Drosophila*. *Development.* 124:2409–2419.
- Mitchison, T., L. Evans, E. Schulze, and M. Kirschner. 1986. Sites of microtubule assembly and disassembly in the mitotic spindle. *Cell.* 45:515–527.
- Moutinho-Santos, T., P. Sampaio, I. Amorim, M. Costa, and C.E. Sunkel. 1999. In vivo localisation of the mitotic POLO kinase shows a highly dynamic association with the mitotic apparatus during early embryogenesis in *Drosophila*. *Biol. Cell.* 91:585–596.
- Nakaseko, Y., G. Goshima, J. Morishita, and M. Yanagida. 2001. M phase-specific kinetochore proteins in fission yeast. Microtubule-associating Dis1 and Mtc1 display rapid separation and segregation during anaphase. *Curr. Biol.* 11:537–549.
- Nigg, E.A. 2001. Cell division: mitotic kinases as regulators of cell division and its checkpoints. *Nat. Rev. Mol. Cell Biol.* 2:21–32.
- Ohkura, H., M.A. Garcia, and T. Toda. 2001. Dis1/TOG universal microtubule adaptors—one MAP for all? *J. Cell Sci.* 114:3805–3812.
- Pasqualone, D., and T.C. Huffaker. 1994. *STU1*, a suppressor of a β -tubulin mutation, encodes a novel and essential component of the yeast mitotic spindle. *J. Cell Biol.* 127:1973–1984.
- Pierre, P., J. Scheel, J.E. Rickard, and T.E. Kreis. 1992. CLIP-170 links endocytic vesicles to microtubules. *Cell.* 70:887–900.
- Pfarr, C.M., M. Coue, P.M. Garissom, T.S. Hays, M.E. Porter, and J.R. McIntosh. 1990. Cytoplasmic dynein is localized to kinetochores during mitosis. *Nature.* 345:263–265.
- Rieder, C.L., and G. Cassels. 1999. Correlative light and electron microscopy of mitotic cells in monolayer cultures. *Methods Cell Biol.* 61:297–315.
- Rieder, C.L., S.P. Alexander, and G. Rupp. 1990. Kinetochores are transported poleward along a single astral microtubule during chromosome attachment to the spindle in newt lung cells. *J. Cell Biol.* 110:81–95.
- Saunders, W.S., V. Lengyel, and M.A. Hoyt. 1997. Mitotic spindle function in *Saccharomyces cerevisiae* requires a balance between different types of kinesin-related motors. *Mol. Biol. Cell.* 8:1025–1033.
- Saunders, W.S., and M.A. Hoyt. 1992. Kinesin-related proteins required for structural integrity of the mitotic spindle. *Cell.* 70:451–458.
- Shah, J.V., and D.W. Cleveland. 2000. Waiting for anaphase: Mad2 and the spindle assembly checkpoint. *Cell.* 103:997–1000.
- Sharp, D.J., H.M. Brown, M. Kwon, G.C. Rogers, G. Holland, and J.M. Scholey. 2000a. Functional coordination of three mitotic motors in *Drosophila* embryos. *Mol. Biol. Cell.* 11:241–253.
- Sharp, D.J., G.C. Rogers, and J.M. Scholey. 2000b. Microtubule motors in mitosis. *Nature.* 407:41–47.
- Sharp, D.J., G.C. Rogers, and J.M. Scholey. 2000c. Cytoplasmic dynein is required for poleward chromosome movement during mitosis in *Drosophila* embryos. *Nat. Cell Biol.* 2:922–930.
- Whitfield, W.G., S.E. Millar, H. Saumweber, M. Frasch, and D.M. Glover. 1988. Cloning of a gene encoding an antigen associated with the centrosome in *Drosophila*. *J. Cell Biol.* 89:467–480.
- Williams, B.C., T.L. Karr, J.M. Montgomery, and M.L. Goldberg. 1992. The *Drosophila l(2)zw10* gene product, required for accurate mitotic chromosome segregation, is redistributed at anaphase onset. *J. Cell Biol.* 118:759–773.
- Wood, K.W., R. Sakowicz, L.S. Goldstein, and D.W. Cleveland. 1997. CENP-E is a plus end-directed kinetochore motor required for metaphase chromosome alignment. *Cell.* 91:357–366.
- Yao, X., A. Abrieu, Y. Zheng, K.F. Sullivan, and D.W. Cleveland. 2000. CENP-E forms a link between attachment of spindle microtubules to kinetochores and the mitotic checkpoint. *Nat. Cell Biol.* 2:484–491.